Int J Mater Form (2009) Vol. 2 Suppl 1:25–28
DOI 10.1007/s12289-009-0536-3
© Springer/ESAFORM 2009

ADVANCES IN FORCE MODELLING FOR SPIF.

R. Aerens [1], J.R. Duflou [1], P. Eyckens [2], A. Van Bael [2]

[1] K.U.Leuven (PMA),
Joost.Duflou@mech.kuleuven.be, Celestijnenlaan 300b, B3001 Heverlee, Belgium T: +32 16 32 28 45,
[2] K.U.Leuven (MTM),

ABSTRACT: The aim of the study was to establish practical formulas allowing to predict the forces occurring during the process of Single Point Incremental Forming (SPIF). This study has been based on a large set of systematic experiments on one hand and on results of FEM simulations on the other hand. This led to analytical formulas allowing to compute the three main components of the force for five selected materials in function of the working conditions (sheet thickness, wall angle, tool diameter and step down) with a good precision. Moreover a general model has been deduced allowing to compute an approximate value for the force for any material, based on knowledge of the tensile strength only.

KEYWORDS: "Single Point Incremental Forming", forces, material, thickness, working conditions

1. INTRODUCTION

Single point incremental forming (SPIF) is a variant of incremental forming in which flat metal sheets are gradually formed into 3D shapes using a generic tool stylus only. This new forming method is especially suitable for small batch production and rapid prototyping of sheet metal parts.
The control of the incremental forming process requires a good knowledge of the forming forces: it can contribute to the preservation of the tooling and the machinery used in the process, but is especially of fundamental importance when using a robot as forming platform. Indeed, a robot is typically not a stiff structure and due to the forming forces, the device deflects, causing important deviations to the tool path which result in errors in the geometry of the achieved parts. An important step for solving this problem is to include compensation for the deflection to be expected in the tool path. This is possible on two conditions, firstly the stiffness of the robot has to be known in all its configurations, and secondly, the forces need to be predicted with sufficient accuracy. Force prediction is the topic of this paper.

2. THE FORCE MEASUREMENT METHOD

The forces were mainly studied in steady state and therefore they were observed during the forming of cones. With the test platform, the three components of the force: the axial force *Fz*, and *Fx* and *Fy* (parallel to the x and y axis of the machine) (Figure 1) were measured.
For making a cone, consecutive circular toolpaths are executed which yields a stable signal for *Fz* and two sinusoidal signals for *Fx* and *Fy*. The vector sum of those two values is the in-plane force *Fxy,* which is stable, and the angle ψ between *Fx* and *Fxy* is known. Using the force pulse generated by the depth increment, the position of the tool can determined on the circumference (angle θ). With those data the two main components of the in-plane force i.e. the radial and tangential components *Fr* and *Ft* (Figure 2) were computed. For a depth increment given in position (-x,0) as shown in Figure 1:

$$Ft = sign(Fx)\, Fxy \sin(\theta + \psi) \qquad (1)$$

$$Fr = -sign(Fx)\, Fxy \cos(\theta + \psi) \qquad (2)$$

These forces are related to the length of the generating line of the cone g (Figure 1). For the axial force we retained two values: its peak value (when present) *Fz_p* and its steady state value *Fz_s* (resp. 2700 N and 2450 N in the example shown in Figure 2).

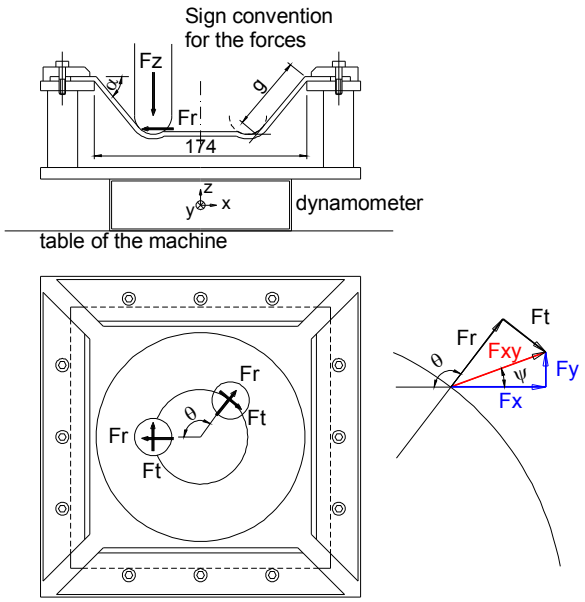

Figure1: *Sketch of the rig mounted on the dynamometer and the relation between Fx, Fy and Ft, Fr.*

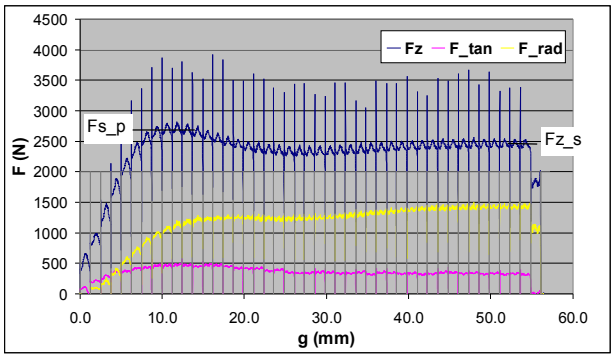

Figure 2: *Typical record of the three components of the process force versus g (DC01 1.15 mm, wall angle 60°, tool diameter 25mm, scallop height 0.015 mm).*

3. THE INVESTIGATIONS

For 5 materials (a soft aluminium alloy: AA3003, an Al Mg alloy: 5754, a deep drawing steel: DC01, a stainless steel: AISI 304 and a spring steel 65Cr2), we studied the influence of the following parameters: the sheet thicknesses (t), the wall angle (α), the tool diameter (d_t) and the scallop height (Δh) (the depth increment (Δz) is related to the scallop height taking in account the tool diameter and the wall angle (Equation 3)) on the forces.

$$\Delta z = 2\sin\alpha\sqrt{\Delta h\,(d_t - \Delta h)} \approx 2\sin\alpha\sqrt{\Delta h\, d_t} \qquad (3)$$

A preliminary study has been conducted with the aim to identify the kind of relation that exists between each parameter and the three components of the force. Therefore, for one material (AA3003), the influence of each parameter has been observed while the other parameters were kept constant, at standard values. The standard values are: tool diameter (d_t) of 10 mm, sheet thickness (t) of 1.2 mm, wall angle (α) of 50° and depth increment (Δz) of 0.5 mm. The tool speed was 2000 mm/min and oil was used as lubricant. A first analysis has been reported in [1]. In a new interpretation of the results, we could state that:

For *Fz_p*, there is a linear relation with all the parameters in logarithmic scale.

For *Fz_s*, there is a linear relation with all the parameters except α in logarithmic scale. *Fz_s* is proportional to ($\alpha \cos \alpha$).

For *Ft*, there is a linear relation with t and Δz in a logarithmic scale. For the chosen standard working conditions *Ft* was nearly constant.

For *Fr*, the value of *Fr* varies from negative values for relatively small wall angles to positive values for larger wall angles.

According to these conclusions, for each material, two series of experiments were planned: firstly, "wall angle tests" for which the sensitivity to α is recorded with small α–increments till failure of the material (the other parameters being kept at standard values) and secondly, "factorial 2^n tests" in which all combination of 2 levels of each parameter (including α) are covered.

For *Fz_p*, *Fz_s* and *Ft*, the aim is to establish regression equations in function of the parameters t, α, d_t and Δh. Since regression equations from factorial 2^n tests are simple linear interpolations between results, the relations between the variables and the parameters have to be linear. This condition is fulfilled when we treat the logarithm of the variables and the parameters except for α.

In order to manage the special sensitivity to α, a new variable has been introduced: *F1,* which is *Fz_s* divided by (α cos α) and the regression equations have been established for *F1* . Finally, the regression equation for *Fz_s* is obtained by simply multiplying the one for *F1* with ($\alpha \cos \alpha$). For the regression equations, only influences and interactions higher than 5 % were taken into account. The regression equations are automatically generated in the format of FORTRAN subroutines (self-developed software).

- For *Fr*, an analytical relation between the *Fr* and *Fz* components will be discussed and the link to the process geometry will be analyzed in Section 5.

4. RESULTS OF THE EXPERIMENTS AND THE RELATED FORCE EQUATIONS

As an example, the results for DC01 are graphically represented in Figures 3 and 4. In Figure 4 *Fz_p* is not shown since in many cases no peak is noticeable. This representation allows to easily visualize the relative importance of the three force components and the

influence of the parameters. The double points close to each other on the graphs correspond to the low and high scallop height (the higher Δh yielding the highest force).

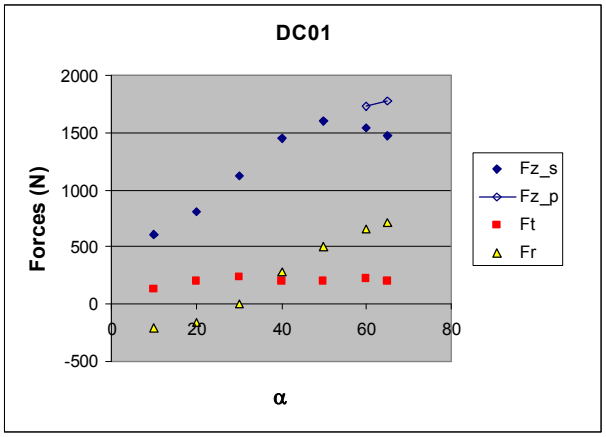

Figure 3: *Influence of the wall angle α on the three force components in steady state and Fz_p for DC01, d_t 10 mm, Δh 0.005 mm.*

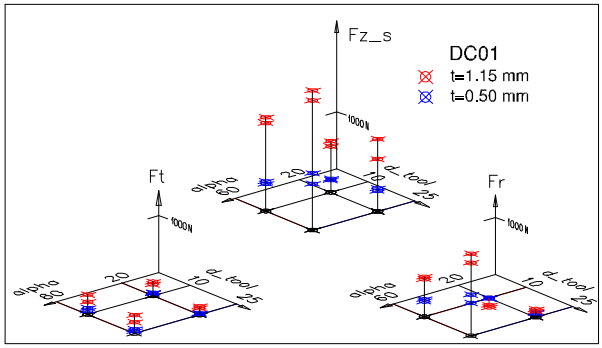

Figure 4: *Influence of the parameters (2 levels) on the three force components in steady state.*

Detailed regression equations were obtained for the five studied materials (not shown). Hereafter the equations for DC01 limited to the factors depending on the direct influences, (which means that the factors depending on interactions of first and higher order are neglected) are shown. So, the regression equations are simple power functions but it results in a larger uncertainty: the largest error is indicated between square brackets in Equations 4 to 6. Note that for *Ft* the error is large, but its absolute value remains small.

In the next formulas α is expressed in degrees.

$$Fz\_s = 16.26\, t^{1.35}\, d_t^{\,0.48}\, \Delta h^{0.12}\, \alpha^{1.11} \cos\alpha \quad \cdots (4)$$

[13.4 %]

$$Fz\_p = 40.7\, t^{1.42}\, d_t^{\,0.48}\, \Delta h^{0.12}\, \alpha^{0.73} \quad \cdots \quad (5)$$

[15.9 %]

$$Ft = 662.1\, t^{1.82}\, d_t^{\,-0.52}\, \Delta h^{0.39}\, \alpha^{0.54} \quad \cdots \quad (6)$$

[33.3 %]

5. RELATION BETWEEN THE RADIAL AND THE AXIAL FORCE COMPONENTS

In order to establish the relation between the radial component and *Fz_s*, we first looked to the results of a number of Finite Element (FE) simulations and in particular to the shape of the contact area between the tool and the sheet and to the distribution of the contact pressure. Detailed results can be found in the work of P. Eyckens [2].

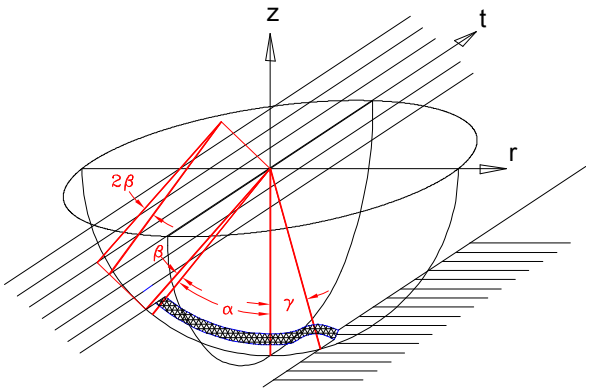

Figure 5: *The modelled contact area and the associated dimensions.*

From these results, we could deduce that the contact area may be approximated by a ribbon of constant width and that the contact pressure has approximately a constant distribution profile along the ribbon.

The length of the ribbon depends on three angles (Figure 5): the scallop angle β (angle comprising a halve "wave" at the surface of the cone (known), the wall angle α (known) and the "groove" angle γ (angle comprising the arc between the top of the tool and the end of contact with the groove at the bottom of the cone). This last angle is important since it can be larger than the actual wall angle. From measurements of the profiles of cones at bottom level, it appears that this angle is mainly depending on the tool diameter and nearly independent of the wall angle. The following equation was found to be a reasonable approximation.

$$\gamma = 0.3\ (d_t / 10)^{-c} \qquad \text{(rad)} \qquad (7)$$

where d_t is the diameter of the tool in mm

$c = 2.54$ for aluminium alloys and DC01

1.20 for AISI 304

Finally, knowing the dimensions of the contact ribbon and assuming a constant contact pressure along this ribbon, a relation has been established between the radial component *Fr* and the axial component *Fz_s*.

$$F_r = F_z \tan\frac{\alpha + \beta - \gamma}{2} \qquad (8)$$

This relation gives a good approximation in many cases but not all. A small correction factor was therefore introduced, formulated as a polynomial deduced from the results of the factorial 2^n tests $P(\alpha, d_t, t, \Delta h)$.

$$F_r = F_z \left[\tan \frac{\alpha + \beta - 0.3\,(d_t/10)^{-c}}{2} + P(\alpha, d_t, t, \Delta h \right] \quad (9)$$

6. GENERALIZED FORMULA FOR THE FZ_S FORCE

Using a common set of process parameters for the different materials (except 65Cr2 since it has been tested in a thickness deviating from the thickness range of the other materials), the corresponding "*reference force Fz_s*" was computed for each material. The common settings are:

- t = 0.9mm: this value was chosen in order to assure minimal extrapolation in the computations (highest thickness for AISI was 0.8 mm and lowest thickness for AlMg3 was 1 mm, see Section 3)
- d_t = 15mm, Δh = 0.010mm, α = 45°: chosen as average values

We can see in Figure 6 that a simple proportionality can be observed between the *reference force Fz_s* and the tensile strength *Rm*. This can be expressed as follows:

$$Fz\_s_{REF}\,(N) = 3.8\,R_m\,(N/mm^2) \quad (10)$$

Since the influence exponents of the parameters in the Fz_s show a limited spread, a generalized formula using averaged exponents and neglecting all the interaction terms, can be considered:

$$Fz\_s \div t^{1.57}\; d_t^{\,0.41}\; \Delta h^{0.09}\; \alpha\, \cos\alpha \quad (11)$$

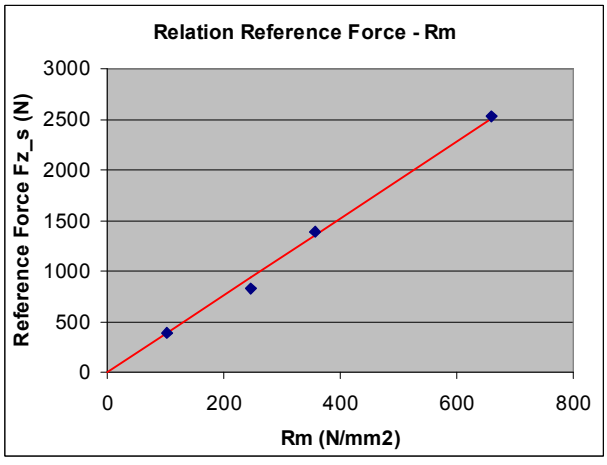

Figure 6: *Proportionality between the "reference force" and the tensile strength Rm.*

Combining Equations (10) and (11), an approximated generalized formula is obtained which allows to predict the axial force *Fz_s* for any material, based on the tensile strength as only required input:

$$Fz\_s = 0.0716\,Rm\,t^{1.57}\; d_t^{\,0.41} \Delta h^{0.09}\; \alpha\, \cos\alpha \quad (12)$$

where *Fz_s* is expressed in N, *Rm* in N/mm², t in mm, d_t in mm, Δh in mm and α in deg.

The precision of this formula has been checked by comparing it with the experimental test results. We can conclude that the probability to make an error smaller than x % can be read from the graph given in Figure7. For example, a relative error of at most 15% is obtained in 77% of all cases.

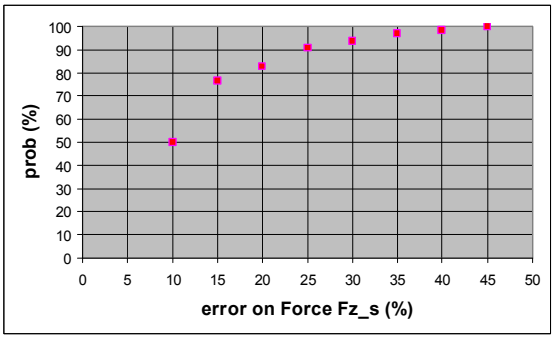

Figure 7: *Relation error-probability of occurrence*

7. CONCLUSION

For five studied materials (AA3003, 5754 (AlMg3), DC01, AISI 304, 65Cr2), regression formulas were obtained that allow to compute the three components of the forming force with a good precision.

Based on an analytical force analysis of the process and on results of FEM simulations, a formula to compute the radial component (*Fz_r*) has been deduced. This component is linked to the value of the axial component *Fz_s*.

For any other material, the use of an approximate formula for the estimation of the *Fz_s* force component is suggested. This estimation method uses the tensile strength of the concerned material as only material specification input parameter.

8. REFERENCES

[1] J. Duflou, Y. Tunçkol, A. Szekeres, P. Vanherck: Experimental Study on Force Measurements for Single Point Incremental Forming, Journal of Materials Processing Technology, Volume 189, Issues 1-3, Pages 65-72, 6 July 2007

[2] P. Eyckens, A. Van Bael, R. Aerens, J. Duflou, P. Van Houtte: Small-scale Finite Element Modelling of the Plastic Deformation Zone in the Incremental Forming Process, Proceedings of *the 11th ESAFORM Conference on Material Forming*, Lyon, April 2008